BASICS OF GRAVITATIONAL WAVE PHYSICS

2022 ICTS lecture by Dr. Bernhard Muller and arXiv:2104.06462v1 by Marek *et al.* (2021)

BRAJESH KUMAR PADHI (Intern)
Faculty of Physics, University of Warsaw
Date of completion of draft: 27/06/2025

Neutrinos & Gravitational Waves from CCSNe

1 Objectives -

1. Basic formulations of GWs.
2. Generation mechanisms of GWs.
3. Various graphical interpretations.
4. Supernova mechanism & evolution.
5. PNS properties & correlations.
6. Supernova simulations.
7. GW data analysis overview.

2 Basic formulations -

GWs arise from acceleration of asymmetric mass distributions like that of BH, NSBH & NSNS binaries or through CCSNe. The strain experienced by a LIGO detector arm during detection of an event can be dimensionally expressed as -

$$h \approx \frac{2G}{c^4 r} \epsilon M R^2 f^2$$

Here,
G = Universal gravitational constant
c = Speed of light in vaccum
r = Distance of source from detector
ϵ = Asymmetry parameter which is obtained from supernova simulations($\epsilon << 1$)
M = Mass involved in supernova
R = Characteristic length/radius of explosion
f = Frequency of explosion

GWs are originated from variation in quadrapole moment. This is possible by 3 broad mechanisms -

1. Permanent deformation/collapse of core due to rotation of progenitor.
2. Convection & SASI in supernova.

3. Triaxial instability due to very fast rotation due to which progenitor becomes a true ellipsoid.

The third mechanisms produces very strong GWs but is highly specific to certain simulations. By very fast rotation, the progenitor achieves instability by easily reaching the required T/W ratio. (T: Rotational energy, W: Binding energy)

3 Generation mechanisms -

3.1 Rotational Bounce Signal -

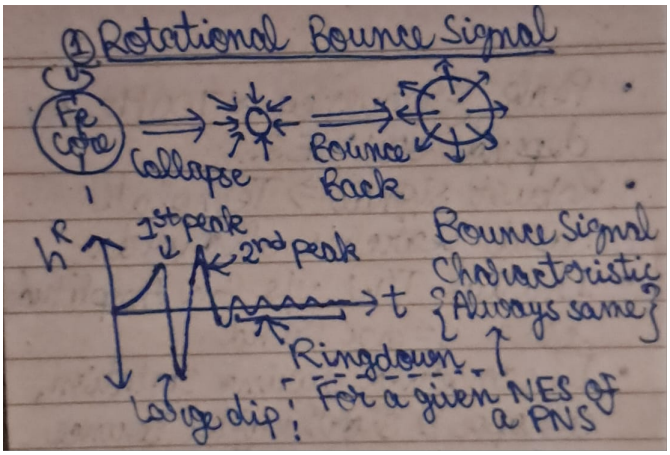

The rotating inner Fe core collapses due to high gravitational pull & bounces back to produce a huge shockwave which initiates the supernova explosion. The usual GW bounce signal (scaled strain(h^R) v/s time) produced has a characteristic consistent waveform for a given nuclear equation of state (NES) for a particular proto-neutron star (PNS) in a particular simulation. It always has the same waveform shape - exponential rise from baseline, then a first peak, followed by a large dip & a higher secondary peak followed by a decaying ringdown signal. The waveform exhibits a higher amplitude in case of higher rotation rate of progenitor. The waveform might be different in exceptional cases when the rotation rate is very very high.
The peak frequency from this signal is usually $\approx 700Hz$ although it highly depends on the NES. If the signal obtained is robust, template based searches are ideal & preferred.
The initial T/W v/s GW amplitude strength follows a linear (y=mx) trend.
The angular momentum of the progenitor is conserved during rotation, collapse & shortly after the initial bounce wrt a particular mass shell (SNRegion).
The resultant PNS after bounce has a non-uniform differential rotation irrespective of Fe core rotation nature.

The general GW stress v/s time signal obtained post bounce from a 2D simulation has some salient

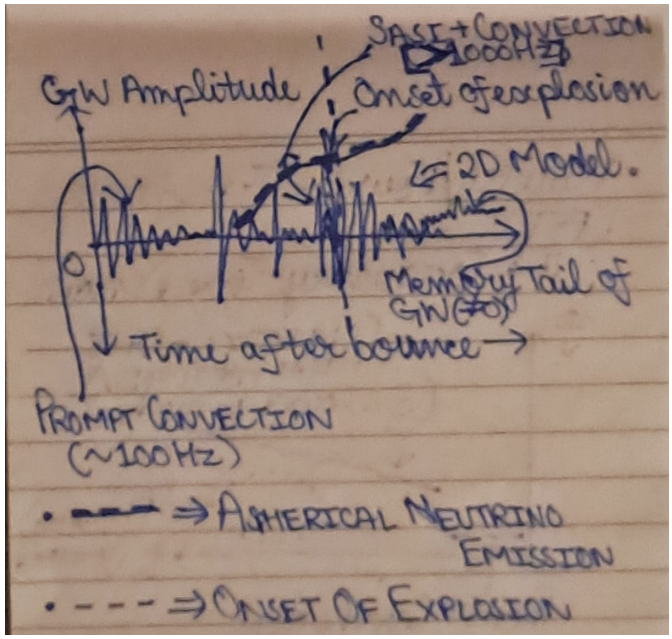

features in increasing temporal order-
1) An initial prompt convection region dominating $\approx 100Hz$.
2) Some regular amplitude fluctuations.
3) SASI+ Convection region dominating few hundreds to $> 1000Hz$ just before onset of explosion.
4)*The aspherical neutrino emission initiates somewhere in the time between prompt convection & SASI regions which thereafter keeps increasing almost exponentially*.
5)The major signal is observed during onset of explosion with frequent changes in the strain values.
6) After the major signal has subsided, a residual memory signal comes into existence whose mean value is not zero.

Typically, the strain-time signal is subjected to a wavelet/fast fourier transform (FFT) so that frequency-time plots are obtained for better visualization. In these plots, three predominant sections are found-
1) Prompt convection - Low frequency, nearly constant frequency, temporally early short signature which is usually produced by excitation of p-modes.
2) Convection+SASI - High frequency, nearly linearly increasing with time, after prompt signature, produced by excitation of f & lower g-modes.
3) SASI - Lower frequency temporally late patch of signal which is produced due to excitation of higher g-modes & strongly detected due to their existence in highest sensitivity region of LVK detectors.

The early & low frequency signal corresponding to a few hundred Hz are generated due to prompt

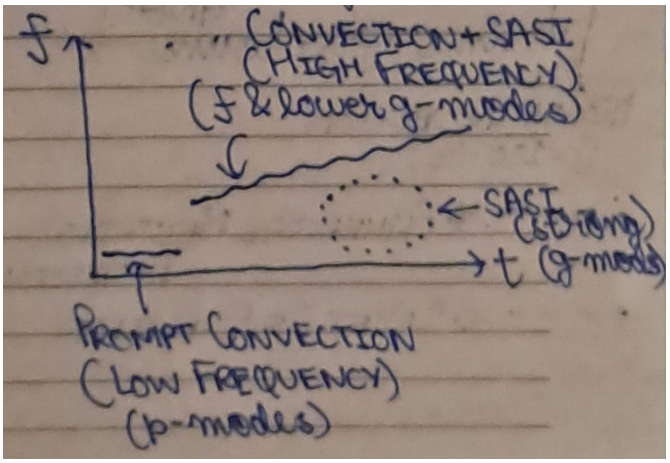

convection after shock.
Convection excites the quadrapolar p-modes (acoustic) which are situated between shockwave & PNS.
Bulk of the signal produced is associated with activity of convection& SASI.
The strongest GW emission occurs around time of shock revival & then gradually subsides.
The tail/memory signal usually occurs due to anisotropic emission of neutrinos & asymmetric expansion of the shock (bounce).

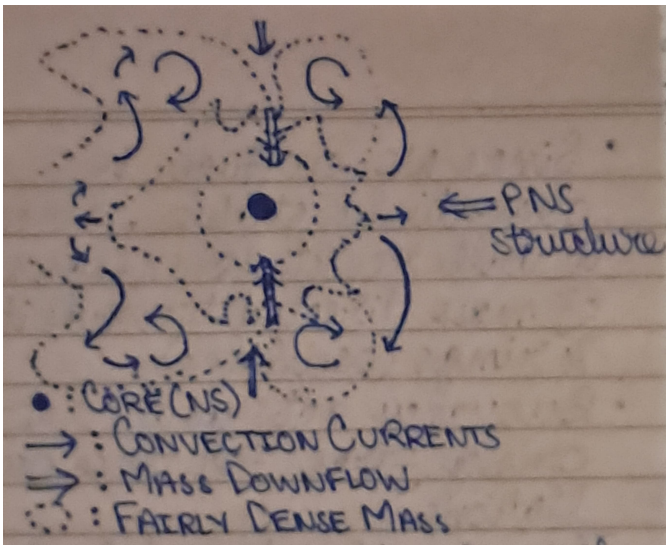

The PNS structure is very exotic & complex. It typically consists of a fairly symmetrical dense central core surrounded with lesser and lesser denser material as we move radially outwards. For a 2d simulation, there tends to be existence of a mirror axis about which the structure is symmetric. The 2d simulations are usually cylindrically symmetric & hence less accurate than spherically symmetric 3d simulations (but require less computation power in comparison to 3d). The PNS has

several layers/regions akin to the onion peel structure. The motion in outer layers becomes more & more complex and non-linear with convection currents determining their movements. There are also regions of heavy mass downflow, wherein mass from outer layer is pushed back onto the core while at regions of heavy mass outflow, the materials are pushed away akin to jets at high speeds away from the core.
Convective currents are the primary agents of excitation of various modes. However, GWs originate only from oscillation modes of PNS.
The inner NS core surface is convectively stable due to high density & thus resists downflow of mass directly towards it and rings/oscillates to counteract it. For these oscillations, buoyancy of turbulent matter acts as a restoring force. This gives rise to fundamental/f-modes & lower order gravity/g-modes at regions of overshooting and/or downflow.

Frequency of modes can be estimated by density and pressure gradients at downflow regions by assuming the PNS to comprise of roughly isothermally stratified atmosphere at its surface vicinity & using the NS parameters as -

$$f \approx 2\pi \frac{GM}{R^2} \sqrt{\frac{1.1 m_n}{< E_{v_n} >}} \text{ x } 1\text{-}\frac{GM}{Rc^2}$$

where,
$\frac{GM}{R^2} = g_n$ which is the acceleration due to gravity at surface of neutron star
$< E_{v_n} >$ is the electron anti-neutrino mean energy that acts as a proxy for PNS surface temperature
$1 - \frac{GM}{Rc^2}$ is the relativistic correction term
The above mentioned correction term arises due to redshifts in GWs.
The usual $< E_{v_n} >$ is of the range of few MeVs.
The time integrated energy radiated by GWs is linearly related to turbulent flux of convective motion that hits a PNS surface -

$$E_{GW} = 3\text{x}10^{43} erg \left[\frac{\int F_{turb} dt}{10^{50} erg} \right]^{1.88}$$

Here,
dt is analogous to duration of convection
$\int F_{turb}$ is analogous to intensity of convection that excites the modes

Usually, more massive progenitor $\implies$ longer accretion in explosion $\implies$ more energetic explosion $\implies$ stronger GWs.
GW emission is sensitive to mass present in the gain region & convective velocities.

Strong GWs are emanated only when the supernova explosion occurs. In the absence of an explosion event, GWs produced are very weak, irrespective of the mass of the progenitor.

SASI stands for Standing Accretion Shock Instability which is an oscillatory instability. In the presence of strong SASI additional low frequency emission in the range of few hundred Hz is observed.
Due to frequency doubling, the frequency of GWs from a progenitor cannot be identified directly & solely from the given SASI frequency of that particular PNS.
The stochastic convection currents excite g-modes which result in production of SASI leading to a coherent fluid motion with a specific period which, in turn, produces strong low frequency GWs.
The presence & absence of SASI can be rather easily qualitatively determined from strain-time

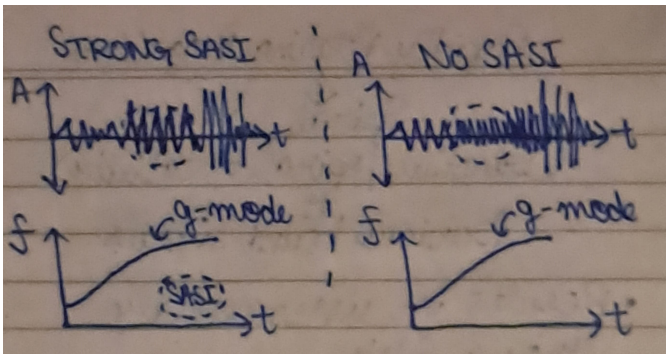

and frequency time maps. The frequency of SASI usually increases with collapse & decreases with expansion.

Rapidly rotating progenitors give rise to spiral modes (from triaxial/spiral instability) along with previously mentioned bound signals (p,f,g-modes). Due to this, unexpectedly strong GWs are observed from a rapidly rotating progenitor.

Except for SASI, most of the GW power is emitted above the optimal sensitivity range for LVK, however, foundational parameters like total energy & peak frequency can be inferred well within plausible error ranges.

Direct usage of GW signals from supernova simulations is not preferred since most of them do not evolve the metric of space-time. Even if they do, the waves' degrees of freedom are too weak. Hence, it is better to post-process the simulation output by quadrapole formula modified with relativistic effects -

$$h^{ij} = \frac{2G}{c^4 D}\frac{\partial^2}{\partial t^2}\left[\int \rho(x^i x^j - \delta^{ij} r^2) d^3x\right]$$

Here, the square bracket term represents the symmetric trace free part of quadrapole moment. Relativistic effects are sizable in supernova core, such that, $\frac{GM}{Rc^2} < 0.1$. However, simulations approximate relativistic gravity by using a modified gravitational potential which is undesirable. Thus, to reduce numerical noise, quadrapole formula is recasted to eliminate one time derivative & relativistic corrections are included. The moment integral is converted such that strain is expressed in terms of density, gravitational acceleration & components of hydrodynamic stress tensor. The boundary condition that is mandatory to satisfy is that the integral should vanish for a perfectly spherical flow.

Spectral properties usually change with time & mostly all simulations end before emission ceases due to high computational costs.

Also, the fourier transform $\bar{h}^{ij}$ is required such that-

$$\bar{h}^{ij}(f) = \int_{-\infty}^{\infty} h^{ij}(t').W(t').e^{-2\pi i f t'} dt'$$

& it is used in computation of ASD & PSD and in elimination of SNR. Here, W(t') is a window function that is either rectangular or with tapering edges to optimize spectral leakage. The presence of a tail/memory signal contaminates the spectrum for analysis and hence it can be eliminated by windowing. However, too much windowing can remove significant emissions at signal ends & suppress the early occurring prompt convection signal.

Spectrograms can be made by STFT such that -

$$\tilde{h}^{ij}(t, f) = \int_{-\infty}^{\infty} h^{ij}(t')W(t' - t)e^{-2\pi i f t'} dt'$$

or wavelet transform such that -

$$\hat{h}^{ij}(t, p) = \frac{1}{\sqrt{p}} \int_{-\infty}^{\infty} h^{ij}(t')\psi\left(\frac{t' - t}{p}\right) dt'$$

where, $\psi()$ is a mother wavelet. Using wavelet transform over a few oscillations is best since PNS & SASI oscillations are coherent for a few cycles at the beginning.

Usually, the EM signals lag behind the GW signals (by some minutes to some hours) for a particular supernova progenitor.

Reference -Neutrinos and Gravitational Waves from Core-Collapse Supernovae (Lecture 3) by Bernhard Müller

Detecting & reconstructing GWs from next galactic CCSN in advanced detector era

1 Overview of basic concepts -

cWB refers to coherent WaveBurst algorithm. It is a preferred way of analysis as it makes minimal assumptions on the morphology of a GW signal.
The detection range for a neutrino driven explosion (NDe) is $\approx 10kpc$ while for a rapidly rotating progenitor it can be $> 100kpc$. For proper detections, the minimum signal to noise ratio (SNR) should be $\approx 10 - 25$.
The most challenging signals to reconstruct are -
1) Long duration NDes.
2) Models forming BH after core bounce (simulations crash as soon as event horizon forms).
Binary black hole (BBH) merger $\implies$ First ever GW signal detected.
Binary neutron star (BNS) merger $\implies$ GW + EM $\implies$ First multi-messenger detection.
A CCSNe is a prominent source of short duration GW transient.
CCSNe occur from massive stars $>\approx 8M_{\odot}$. The explosion mechanism is not fully understood. Further, the origin of asymmetry in the shock is also unclear.
All SNe have been detected till now by EM only & low energy eutrinos observed only for SN1987A.
Usually, neutrinos & GWs leave the PNS core almost around the collapse time.Neutrinos can be used to determine thermodynamic properties of a collapsed core while GWs for dynamics of moving matter in the progenitor.
Due to turbulent flow of matter, CCSNe are stochastic $\implies$ GW time series are stochastic. Hence, the algorithm used for analysis should be flexible enough for large range and/or unexpected GW morphologies.

2 Searches -

1. TAMA 300 + Excess power filter
2. L,V,GEO 600 + Excess power cWB + X pipeline.
3. L,V + cWB.

O1 & O2 used cWB, oLIB & BayesWave. For CCSNe, multidimensional simulations are useful.
Due to stochastic/unpredictability, matched filtering is not used.Hence, PCA, Bayesian inference, ML,etc., are used. Also, weak/minimal assumptions are preferred.

cWB is the only algorithm capable of detecting GWs in low latency. For CCSN search sensitivity → cWB > X-pipeline.
Light squeezing in detectors has increased sensitivity. Also, longer 3D simulations capable of predicting entire Gw signals + better coverage of CCSN parameter space + increase in number of 3D simulations $\implies$ stronger GWs.

3 Objectives -

1. Extensive GW analysis + O4 & O5 predictions.
2. Basic properties, energy evolution, spectra, dominant emission process of predicted GWs are compared.
3. O2 scaled to O4 & O5 used to preserve features of noise.
4. Results assume high significance of events.
5. Challenges of detecting CCSNe physical processes discussed.
6. Reconstruction accuracy of GW morphologies are quantified.

Massive star burns fuel by nuclear fusion which is maximum at core leading to a onion like structure with Fe core at the center. The Chandrasekhar mass limit (M_C) is $\approx 1.4 M_\odot$. If $M_{Fe-core} > M_C$ then due to very high gravitational forces, core collapse occurs leading to formation of a hot PNS; after which it may go for an explosion or collapse into a BH or both combined.
The massive flux of neutrinos from PNS plays a crucial role in explosion leading to I)Neutrino Driven (ND) Mechanism. Neutrinos heat up the matter they pass through, creating a shock which may lead for the star to explode.
There is also a possibility of II)Magneto-rotationally/Magneto-hydrodynamically (MHD) driven mechanism which occurs due to presence of very high progenitor rotation + strong magnetic fields ($\vec{H}$). A seed $\vec{H}$ when combined with the collapse results in a magnified $\vec{H}$ resulting in jets along the rotational axis leading to possible destruction of the star.
There is another mechanism of III) Phase transition (QCD). In this, the accreting matter increases PNS density and temperature leading to the PNS collapse. This results in phase transition to quark matter and a shock dominating the explosion. After this, it can proceed to two fates. In one of them, it goes on to become a CCSNe while in the other, the shock fails and/or matter keeps accreting resulting in a BH formation.
There are also some IV) Extreme Emission models (rare) wherein rapid rotation of progenitor leads to deformation/fragmentation of the PNS then to the CCSNe.
The chance of a CCSNe resulting in a BH formation is $\approx 20\%$. Also, for CCSNe, $\approx 99\%$ of them

are through ND while $\approx 1\%$ are through MHD.

1. Neutrino Driven (ND) mechanism - It has three phases -
   i) Fe core collapse & bounce after reaching threshold nuclear density. Supersonic Fe core collapse + accretion of outer layer leads to initial shock which expands & halts producing a low frequency prompt convection signal followed by a short quiescent/dormant period.
   ii) After 100ms, high neutrino outflow from hot PNS occurs. Neutrinos deposit energy in turbulent matter between PNS & shockwave. It is a crucial mechanism for star explosion to occur. A tug of war between accreting matter & neutrino heating shock goes on for few hundred ms. This can induce ND convection between shock & PNS. Due to neutrino heat + accretion, an oscillating shock is produced, leading to Standing Accretion Shock Instability (SASI) formation. *SASI can be linear (axial) or spiral (circular)*. Aspherical matter movements lead to low frequency SASI/convection GWs (most sensitive to detectors). Eventually, PNS stiffening occurs due to residual electron capture + excitation by accretion. There are three types of restoring forces and their respectively associated modes -
   a) Gravity $\rightarrow$ g-mode
   b) Surface $\rightarrow$ f-mode
   c) Pressure $\rightarrow$ p-mode
   iii) If shock is fully revived, an explosion phase occurs. SASI & convection decay eventually while low rate accretion continues.
2. MHD mechanism - If the progenitor is rapidly rotating, it undergoes MHD leading to a flattened Fe core. This leads to axi-symmetric collapse + strong linearly polarized GW bounce signal.

If shock is not revived in any of the cases, then accretion continues and Bh is formed. The GW signal from simulations cease abruptly when event horizon is formed.
Axisymmetric 2D models produce linearly polarized signals ($h_+ = 0, h_X = 0$), while for 3D models, 2 polarizations h_+ & h_X are available.
EOS can vary from softer to stiffer & may alter GWs. A stiffer EOS means sharper rise in pressure with increase in energy density $\implies$ more resistance to gravitational collapse & compression. A softer EOS means the opposite and it can occur due to phase transitions.
Usually, $3.5M_\odot$ (ultrastripped He star) $\leq M_{star} \leq 60M_\odot$ (all other are ZAMS mass stars).
Star models consider differential rotation & initial central angular velocity (Ω_C).
Energy spectra is used for f_{peak}. The total GW energy, E_{GW} is source angle averaged.
The waveform duration usually extends from time of collapse to time of simulation end. Due to high computational costs, simulations are stoped before full GW formation.

The different waveform families and their properties are summarised in the images.

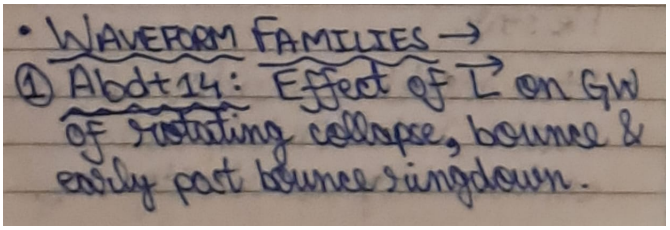

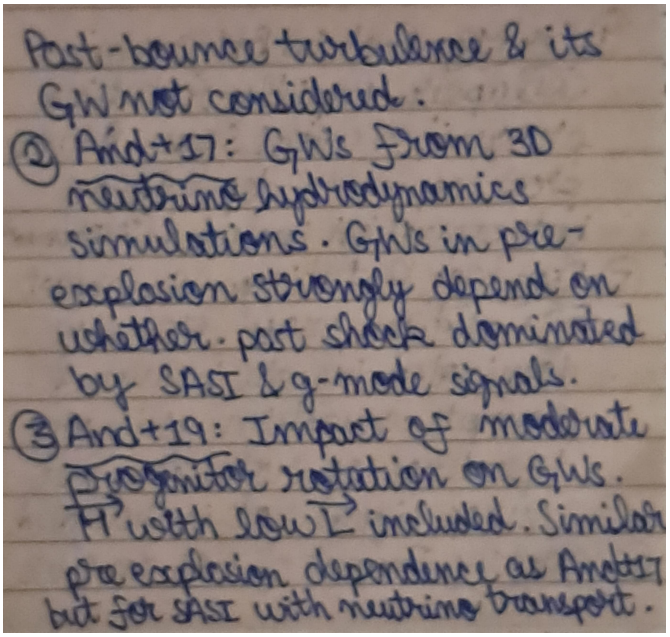

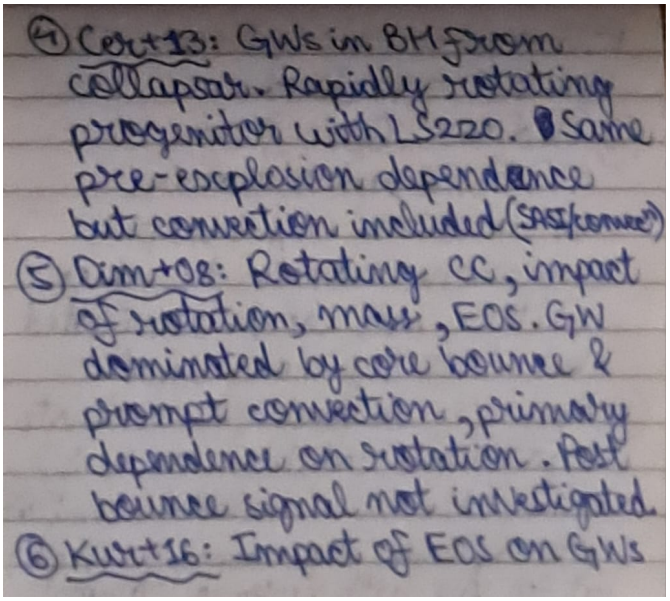

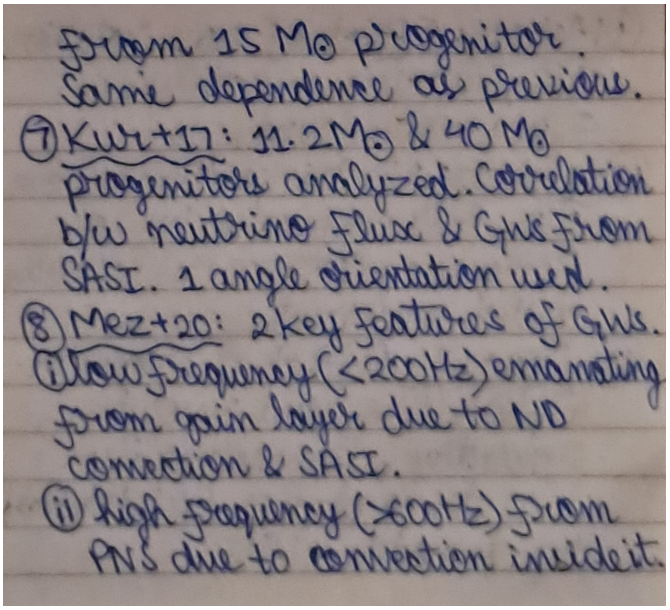

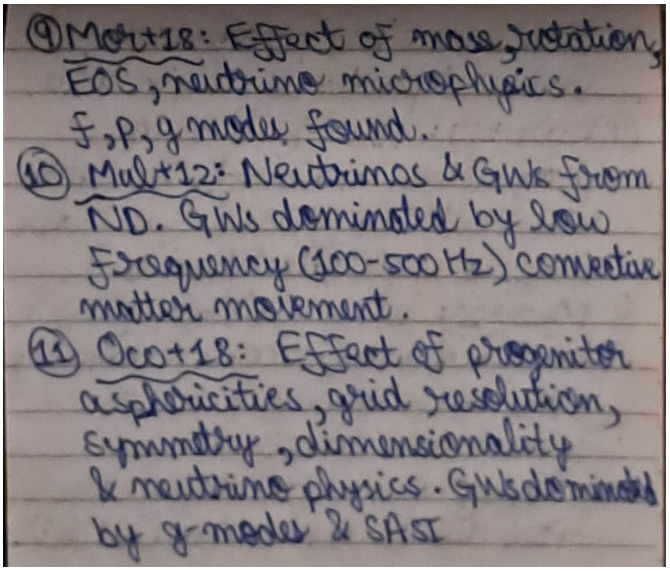

4 GW Calculation & Processing -

Quadrapole approximation is used to extract GWs from accelerating matter in CCSNe.The metric perturbation, $\vec{h}_{ij}^{TT}$ in the traceless transverse (TT) gauge is given by -

$$\vec{h}_{ij}^{TT}(t,\vec{x}) = \frac{1}{D}\ddot{Q}_{ij}\left(t - \frac{D}{c}, \vec{x}\right) : \forall i,j \in [Cartesian]$$

The Q term is a partial time double derivative of traceless quadrapole moment, such that-

$$Q_{ij}(t,\vec{x}) = \frac{2G}{c^4}\int d^3x\rho(t,\vec{x})\left[x_i x_j - \frac{\delta_{ij}|\vec{x}|^2}{3}\right]$$

(12) Ott+13: Focus on post core bounce phase, SASI & ND convection. Just after bounce, cores strongly deformed by prompt convection dominating GWs.

(13) Pow+19: Low & regular CCSNe energies analyzed. Simulation across all evolution phases. g-modes peaking at high frequencies.

(14) Pow+20: Impact of rotation seen.

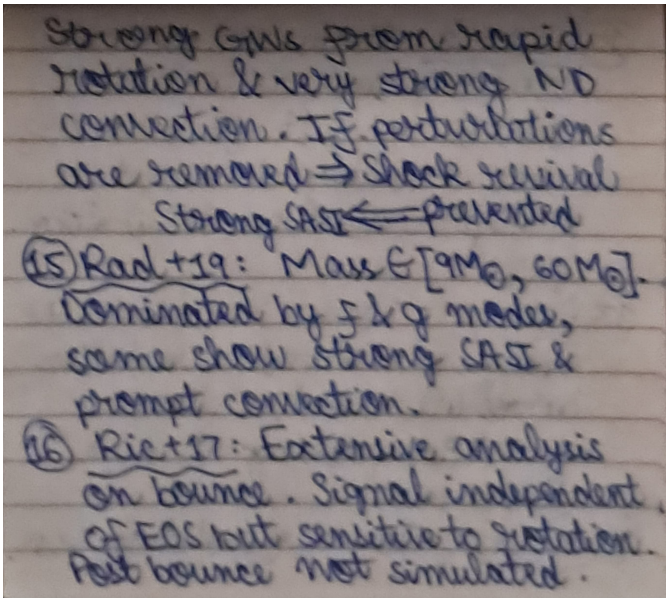

(17) Sch+10: GWs from MHD. Effect of EOS, initial rotation, FT.

(18) Yak+15: Full GW evolution, both low (SASI/convection) & high (g-mode) frequency present.

where, ρ is the mass density of progenitor. Also, $\ddot{Q}_{ij}$ is directly extracted from simulations. The metric can be represented as a linear combination as given in the image -

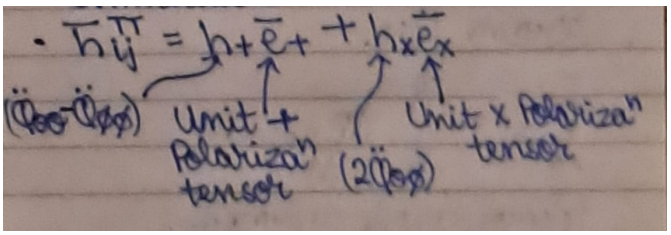

In axisymmetric 2D simulations, $h_X = 0$ hence, Q_{ij} matrix only has diagonal components such that $Q_{11} = Q_{22} = -\frac{1}{2}Q_{33}$ & $h_+ = \frac{3}{2}sin^2\theta.\ddot{Q}_{33}$
The basic GW properties are analyzed from $\ddot{Q}_{ij}$.
Also, the source angle averaged E_{GW} is given by -

$$E_{GW} = \int_{-\infty}^{\infty} \frac{dE_{GW}}{dt}.dt$$

Also, the forier transform is given by -

$$\tilde{Q}_{ij}(f) = \int Q_{ij}(t)e^{-i2\pi ft}$$

The characteristic strain is given by -

$$h_{char} = \frac{1}{D}\sqrt{\left[\frac{2G}{\pi^2 c^3}.\frac{dE_{GW}}{df}\right]}$$

The peak frequency corresponds to maxima of $\frac{dE_{GW}}{df}$
The typical explosion energy is around $10^{51}ergs$.
The $f_{peak} \in [300Hz, 1000Hz]$, $E_{GW} \in [10^{-10}, 10^{-7}].(M_\odot c^2)$ & usually, $E_{GW} < 0.01\% E_{CCSNe}$.
Low frequency ($< 10Hz$) signals are found to exist due to truncation of simulations & lead to discontinuities due to which they are removed by a high pass filter to 10Hz cutoff.
The signals are then resampled to 16384Hz & rescaled to 10kpc.

5 Energy & spectra of GWs -

Gw energies from CCSNe are orders of magnitude weaker than that from BBHs. Due to rapid rotation/fragmentation, a maximum of $\approx 10^{-3}M_\odot c^2$ can be generated from a CCSNe; which is

not usually seen due to them being ND and MHD driven with far less rotation.
Majority of energy of GWs is emitted in higher frequency ranges. The dominant emission is typically from PNS oscillations. The GW detector sensitivities are frequency dependent. Hence oscillations result in peaks in less sensitive region while signals from SASI have highest sensitivity.

6 cWB -

It is an excess power search algo. to detect & reconstruct GWs using minimal assumptions on signal morphologies. cWB does a wavelet transform of strain data by superimposing signals above noise threshold and identifying coherent events. Also,

$$\eta_c = \sqrt{\left[\frac{E_c}{max(\chi^2, 1)}\right]}$$

where, η_c = cWB events ranking stats. $\approx$ SNR, E_c = coherent network energy & χ^2 is the quantitative agreement of reconstructed and original GWs.

$$\chi^2 = \frac{E_n}{N_{df}}$$

where, E_n = residual energy & N_{df} is the number of independent coefficients used. For $\chi^2 > 2.5 \implies$ event rejected.

$$c_c = \frac{E_c}{E_c + E_n}$$

Events accepted when $c_c > 0.5$.

7 Noise rescaling -

Non-gaussian noise dominated high fluctuating data. Noise features are made sure to be preserved while scaling such that -

$$S_{Oi}(f) = S_{O2}(f).\frac{S_{Oi,proj}(f)}{S_{O2,avg}(f)}$$

where, $i \in [AnyRun]$. Phase preserved and spectrum retransformed into time domain.

8 Background estimation -

Time shifting analysis used. Data of one detector is shifted by integral seconds wrt other that is longer than GW time lag between detectors assuring any event detected is noise $\implies$ False Alarm Rate (FAR) found.
Two mutually exclusive classes formed, C1 with short duration O(10)ms blips morphologically similar to CCSN bursts & C2 with other noises.

9 Sensitivity studies -

Waveform from different angles placed randomly in sky with injected noise every 150s & reconstructed with cWB. Detection range = Distance for 50% detection efficiency. Similar method for SNR. Minimum detectable SNR = SNR for 50% detection efficiency. Events with FAR $> 1/year$ are discarded.

10 Results -

For waveforms of 3D simulations, detection efficiency $> 90\%$ while $\approx 70\%$ for linearly polarized GWs. HL network senstive to mostly one of the polarization due to them being nearly parallel. For ND driven explosions, the maximum detection range is around 10kpc. For MHD, range exceeds large magellanic cloud. If amplitudes of turbulent phase are comparable to core bounce then range of MHD detection are even higher.
Short narrowband signals (BBH) are easier to detect by cWB than long/fragmented ones(CCSN). Rapid plumes of infalling matter can also generate broadband GWs, also, SASI & PNS oscillation signals might be disconnect in time-frequency. Usually, minimum detectable SNR $\in [10, 25]$. GWs from ND have higher minimum SNR. If faster BH formation $\implies$ smaller SNR.

11 Reconstruction accuracy -

To quantify accuracy of cWB reconstruction, waveform overlap seen between detected $\vec{w} = w_k(t)$ & injected $\vec{h} = h_k(t)$ such that -

$$O(\vec{w}, \vec{h}) = \frac{(\vec{w}|\vec{h})}{\sqrt{\vec{w}|\vec{w}}\sqrt{\vec{h}|\vec{h}}}$$

where the scalar product is defined as -

$$(\vec{w}|\vec{h}) = \sum_k \int_{t_1}^{t_2} w_k(t) h_k(t) dt$$

for k being detector number and $[t_1, t_2]$ is time range of reconstructed event. O $\in [-1, 1]$ (sign mismatch, perfect reconstruction). Even for stronger signals, waveform overlaps do not reach 0.9 on average. Reconstruction accuracy decreases with waveform length and complexities & lowest for ND waveforms.

At SNR of 20, $f_{peak} \approx 100Hz$ for cWB reconstruction. f_{peak} of a GW corresponds to dominant emission processes. For weak GWs, f_{peak} of a dominant GW emission is reconstructed & with increase in SNR other parts get reconstructed as well. For most ND waveforms, PNS oscillations dominate amplitudes and minimum detectable SNR ≈ 20. The time-frequency path of increasing peak frequency of PNS oscillations becomes visible around SNR 30-40. SASI/convections is reconstructed as well at this SNR.

GWs dominated by SASI/convection are narrow-band & minimum SNR is usually smaller for waveforms dominated by PNS oscillations. Prompt convection signals are also short & reconstructed accurately for small SNR. GWs from rapidly rotating progenitors are dominated by bounce and prompt convection $\implies$ short waveforms $\implies$ SNR ≈ 15. Reconstruction of long signals from BH formation are most difficult $\implies$ SNR ≈ 50.

Reference -Marek *et al.* (2021)